THE LUNAR ORBITER PROJECT SELENODESY EXPERIMENT

By William H. Michael, Jr., and Robert H. Tolson

NASA Langley Research Center
Langley Station, Hampton, Va., U.S.A.

Presented at the Second International Symposium on
"The Use of Artificial Satellites for Geodesy"

Athens, Greece
April 27-May 1, 1965

THE LUNAR ORBITER PROJECT SELENODESY EXPERIMENT

By William H. Michael, Jr., and Robert H. Tolson

NASA Langley Research Center

INTRODUCTION

The Lunar Orbiter Program is one of three United States unmanned lunar exploration programs designed to advance scientific knowledge of the moon and its environment, and to provide engineering and mapping data in support of future manned lunar landings. The highly successful Ranger flights have produced the first close-range photographs of the lunar surface, and have provided new detailed information on lunar topography. The Surveyor spacecraft will soft-land on the lunar surface, and will analyze the dynamics of lunar touchdown, perform lunar surface bearing tests, and transmit detailed TV pictures of the area surrounding the spacecraft. The Lunar Orbiter will be the United States' first close satellite of the moon, and will transmit high-resolution photographs of considerable areas of the lunar surface which will be used for mapping and for selecting landing sites for unmanned and manned spacecraft. The Lunar Orbiter will also carry instrumentation for measuring micrometeroid flux and high-energy particle flux near the moon.

The Lunar Orbiter flights will provide an opportunity, perhaps the first opportunity, for significant improvement in knowledge of the lunar gravitational field through analysis of the tracking data from a close lunar satellite. These new data on the lunar gravitational field will be of considerable interest to scientists concerned with the origin of the moon and the earth-moon system, the internal composition of the moon, and related problems. The knowledge of the gravitational field will also enable precise determination of lunar satellite

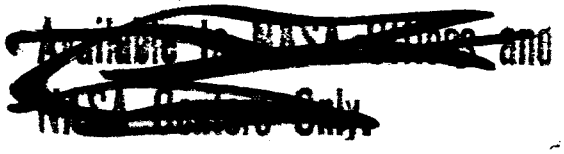

ephemerides, which in turn will contribute to the analysis of the photographic data for selenodetic purposes.

Overall policy direction of the Lunar Orbiter Program is provided by the Office of Space Sciences and Applications, Lunar and Planetary Programs, at NASA Headquarters. Technical project management and direction has been assigned to the NASA Langley Research Center, which has the overall responsibility for project implementation. A prime contractor has been selected to provide the spacecraft and auxiliary ground equipment, to perform associated analyses, and to be responsible for integration of spacecraft subsystems. Tracking and telemetry data from the spacecraft will be acquired through the NASA Deep Space Network, operated by the Jet Propulsion Laboratory. It has been proposed that responsibility for analysis of the tracking data for determination of the lunar gravitational field parameters and other astrodynamic constants be assigned to a team composed of members of the technical staffs of the Jet Propulsion Laboratory and the Langley Research Center. Prompt, preliminary determinations of parameters will be utilized in mission planning for the Lunar Orbiter, and more comprehensive determinations will be performed for general use by the scientific community. If sufficient interest is indicated by other investigators, consideration will be given to procedures for making the tracking data available to them for their own analyses.

Current funding for the Lunar Orbiter makes provision for five flights, which will be primarily designed for photographic coverage of the lunar surface. The parameters of the lunar orbit of the spacecraft will be specified to accommodate the photographic coverage, and therefore will not constitute a set which is ideally suited to determination of the gravitational field, particularly with respect to inclination of the orbits. Nevertheless, preliminary analyses

indicate that considerable improvement in knowledge of the gravitational field will be obtainable. There is also the possibility that additional flights may be scheduled later, and these may well provide more variety in orbital parameters.

DESCRIPTION OF THE LUNAR ORBITER SPACECRAFT AND MISSION

A schematic drawing of the mission profile for a typical Lunar Orbiter flight is shown in figure 1. The vehicle will be launched from Cape Kennedy by an Atlas-Agena booster vehicle, and will be injected into an earth parking orbit. After coasting to the proper position in the parking orbit the Agena engine will be reignited to inject the spacecraft into the translunar trajectory, in which it coasts to the vicinity of the moon. Up to two midcourse corrections may be made to place the spacecraft at the desired point with respect to the moon. Near the position of closest approach to the moon, a retrorocket will be fired to place the spacecraft in an initial lunar orbit. After a number of orbits, during which the initial orbital properties will be determined, the rocket will be fired again to establish the final orbit for taking the photographs. This final orbit will have a relatively low inclination to the lunar equator, nominally about 15°, and will have nominal pericentron and apocentron altitudes of 46 and 1850 kilometers, giving an eccentricity of 0.34, and an orbital period of about 3.5 hours.

The parameters of the nominal orbit are specified to satisfy the requirements of the photographic mission. The area of the lunar surface of primary interest in site selection for early manned landings is shown in figure 2. This area is bounded within $\pm 5^{\circ}$ in latitude and $\pm 45^{\circ}$ in longitude, relative to the lunar equator and the intersection of the mean earth-moon line. An orbit with

low inclination is required to provide side overlap for photographs from successive orbits to achieve continuous coverage. The pericentron altitude directly affects the resolution of the photographs, so a low altitude is desirable; and the orbital period is chosen to provide a sufficient ratio of time in sunlight to time in shadow to satisfy spacecraft power requirements.

Two camera lenses in the spacecraft provide nominal lunar surface photographic resolution of 1 meter for the high-resolution, 95-mm focal-length lens, and 8 meters for the medium-resolution, 16-mm focal-length lens, from the 46-km altitude. Surface coverage provided by a single flight is 40,000 sq km at 8-meter resolution and 8,000 sq km at 1-meter resolution. The coverage is illustrated in figure 2. Several different schemes of overlapping coverage in the high-or-medium-resolution mode can be used. The overlapping coverage, in effect, provides data for stereoscopic analysis. The photographs are taken on film which is developed in the spacecraft, then scanned, and the data transmitted to earth for reconstruction. Additional details on the photographic system and surface coverage can be found in reference 1.

A sketch of the Lunar Orbiter spacecraft is shown in figure 3. Identifiable components are the solar panels, the photographic camera package, the rocket engine and tankage, the high-gain antenna, and the omnidirectional (low-gain) antenna, which will be used for tracking data transmission from the spacecraft. Additional communication and power equipment, a transponder, the flight programer, sensors, and other equipment are situated around the photographic package. The attitude control system maintains the spacecraft in the cruise mode with the longitudinal axis directed toward the sun and the other reference axis directed toward Canopus, a first-magnitude southern hemisphere star. For execution of thrusting maneuvers and for taking a set of photographs, the

spacecraft is oriented in the proper direction by the attitude control jets, on ground command, with use of the inertial reference unit. On completion of the thrusting maneuver or after taking a set of photographs, the spacecraft is reoriented to the cruise mode.

The attitude control jets which produce torques about the yaw and pitch axis are not coupled, and thus will produce small translational accelerations. During the photographic phase of the mission, the translational accelerations produced in maintaining fairly precise control on the cruise orientation and in orienting the spacecraft for sets of photographs may introduce small perturbations in the orbit, so that gravitational parameters determined during the photographic phase of the mission may be subject to small biases. The photographic phase, including transmission of all photographic data back to earth, is expected to be completed within about 30 days. After this time, the accuracy with which the longitudinal axis is oriented toward the sun will be relaxed. Perturbations introduced by the attitude control jet accelerations will thus be decreased, and preliminary analyses indicate that the effects of these perturbations on the determination of the gravitational parameters during the postphotographic phase will be rather small. Nevertheless, consideration is being given to utilizing the attitude control system telemetry data as a means to account for the control jet accelerations and thus to account for these perturbations in the parameter determinations.

The spacecraft will be tracked during the translunar trajectory and in lunar orbit by the tracking stations of the NASA Deep Space Instrumentation Facility, located at Goldstone, California; Woomera, Australia; Johannesburg, South Africa; and Madrid, Spain. Range and range rate (two-way Doppler) data will be obtained through use of a transponder in the spacecraft, operating at

S-band frequency (approximately 2200 megacycles per second). Angular data at the lunar distance is not of sufficient accuracy for tracking purposes and will not be considered here. Use of S-band frequency in the tracking system, and provision for increased accuracy in computing schemes in the orbit determination procedures will result in better data accuracies than those obtained in recent Ranger flights, as reported in references 2 and 3. An estimate of the one-sigma noise level for tracking data for the Lunar Orbiter is 0.002 meter per second in range rate and 10 meters in range.

Tracking data will be received almost continuously during the photographic phase of a mission, to provide data for orbit determination and for control of the spacecraft for photography. For approximately 30 days after the end of the photographic phase, the data cycle will be decreased somewhat, but will provide tracking data for approximately one-half the total orbits per day. For the remainder of the operating lifetime, nominally 1 year, tracking data will be requested for about two orbits per day, 2 or 3 days per week. Preliminary analyses indicate that this tracking schedule should be sufficient for determination of the gravitational field parameters.

DETERMINATION OF GRAVITATIONAL FIELD PARAMETERS

Technical Approach

The main objective of the selenodesy experiment is to determine the coefficients in the expansion of the lunar gravitational potential in terms of spherical harmonics:

$$U = \frac{\mu}{r}\left[1 + \sum_{n=0}^{\infty}\sum_{m=0}^{n}\left(\frac{R}{r}\right)^{n} P_{n,m}(\sin \phi)\left(C_{n,m} \cos \lambda m + S_{n,m} \sin \lambda m\right)\right]$$

where μ is the product of the gravitational constant and the mass of the moon, R is the radius of the moon, r is the radial distance, $P_{n,m}$ are the associated Legendre polynominals, ϕ is latitude, and λ is longitude. This formulation is similar to that used by Kaula in reference 4, but includes the zero degree coefficient $C_{0,0}$ to account for the difference in lunar mass from an assumed value incorporated in μ, and the first degree coefficients to account for the differences between the origin of coordinates and the center of mass. The determination of the coefficients $C_{n,m}$ and $S_{n,m}$ is to be accomplished through analysis of the tracking data from a lunar satellite. Other parameters to be determined in the analysis are noted below.

Two general approaches to the determination of gravitational constants arise from a distinction in use of short-period or long-period and secular perturbations for the analysis. For a short-period analysis, the accelerations of the satellite are utilized in a direct manner in that they are formulated in terms of the observational data, and partial derivatives, of each observation with respect to each parameter to be determined, are used in the differential correction process. For a long-period or secular analysis, the observations may be used to determine a set of "mean" elements and the long-period and secular variations in the elements are analyzed to determine the parameters of interest. In determination of the gravitational field of the earth, the zonal harmonics are best determined by analysis of long-period and secular effects, while the tesseral harmonics are determined by use of short-period effects, as pointed out, for example, in reference 5. For the moon, because of its relatively slow rotation about its axis, tesseral harmonics as well as zonals should be determinable from analysis of long-period effects. Therefore, there is an option available in the lunar gravitational field determination in that either

short-period or long-period and secular analyses may be used. Some preliminary analyses comparing the two methods are presented in a later section. Present plans for the data analysis include provision for performing the analyses by both methods.

For the determination of the gravitational and other parameters of interest, the procedures of differential correction and weighted least squares (with a priori statistics) will be used in the development of suitable computational programs. With this formulation for the "direct" procedure, the quantity to be minimized in the least squares sense is

$$Q = \left[\varphi - \varphi(p)\right]^T W \left[\varphi - \varphi(p)\right] + \Delta p^T \phi^{-1} \Delta p$$

where

$$\varphi(p) = \varphi\left(p_1\right) + A\,\Delta p$$

and where φ is an n-rowed vector of observed tracking data; $\varphi\left(p_1\right)$ is an n-rowed vector of calculated tracking data (based on initial values of the parameters, p_1); A is an nxm matrix of partial derivatives of observables with respect to the m parameters $\left(\frac{\partial \varphi(p_1)}{\partial p_1}\right)$; Δp is the vector of differences between the present estimates and the previous estimates of the parameters, $\left(p - p_1\right)$; W is a diagonal matrix of weights on the observations; and ϕ is the covariance matrix on the a priori estimates of the parameters. On performing the minimization of Q, the m normal equations for corrections to the parameters become

$$\left(A^T W A + \phi^{-1}\right)\Delta p = A^T W\left[\varphi - \varphi\left(p_1\right)\right]$$

These equations yield a solution for the parameters

$$\hat{p} = p_1 + \left(A^T W A + \phi^{-1}\right)^{-1} A^T W \left[\varphi - \varphi(p_1)\right]$$

The solution is iterated by successive substitution of the values of p, obtained from the above equation, for p_1 in the minimization process and in the right side of the above equation until the solution has converged, each time weighting the a priori estimate according to its covariance matrix ϕ. The values of p obtained in the final iteration are then the best estimates of the set of parameters, and the covariance matrix on the parameter set is the $m \times m$ matrix

$$C = \left(A^T W A + \phi^{-1}\right)^{-1}$$

The set of parameters p includes the six parameters defining the state of the spacecraft, the lunar gravitational harmonics, tracking station locations, solar radiation pressure coefficients, the velocity of light, control jet and gas leak forces, and instrument and measurement biases. Provision will exist for determination of any subset of the total set of parameters.

Development of the necessary computational programs for the determination of the parameters is currently in progress. In general, numerical integration techniques (Cowell's method) are being utilized for integration of the equations of motion for orbit prediction, and for calculation of the partial derivatives in the normal equations. Prior to the completion of the computer program developments for determination of parameters, and prior to the receipt of tracking data from a lunar orbiter, sensitivity studies and parameter accuracy estimations can be made using analytical methods and auxiliary computer programs. Some preliminary results of such studies are discussed in later sections.

Brief Review of Present Knowledge

Present knowledge of the lunar gravitational field consists of determination of the mass of the moon and the coefficients of the second-degree harmonics. The lunar mass, in the form of the earth-moon mass ratio, has been determined by measurements of the lunar inequality; a recent determination has been made using observations from the Mariner II Venus mission (ref. 6). The lunar mass has also been determined very recently by analysis of the effect of the lunar gravitational field on the Ranger VI and Ranger VII trajectories (refs. 2 and 3). The Mariner and Ranger determinations are compared in reference 3. A comparison of the differences between these two different methods for determining the mass of the moon may be taken as an indication of the present uncertainty, which amounts to about 2 or 3 parts in 5×10^4 (the value of GM_{moon} obtained from Mariner II is 4902.778 ± 0.3 km^2/sec^3 and from Ranger VII is 4902.580 ± 0.17 km^2/sec^3). This is considered to be a fairly precise determination of the lunar mass, but it should be improved by at least an order of magnitude by analysis of data from the Lunar Orbiter.

The coefficients of the second-degree harmonics are determined from the values of the lunar moments of inertia based on measurements of the physical librations of the moon. Tentative values adopted for use in trajectory calculations as given in reference 7 are equivalent to $C_{2,0} = -2.071 \times 10^{-4}$ and $C_{2,2} = 2.072 \times 10^{-5}$. Estimates of the uncertainties in these values are about 1×10^{-5} or 2×10^{-5} in $C_{2,0}$ and perhaps about 1×10^{-5} in $C_{2,2}$, so that these values should also be improved considerably by analysis of the Lunar Orbiter tracking data.

Tracking Data Sensitivity to Typical Parameters

As an illustration of the feasibility of determination of lunar gravitational coefficients with tracking data of the accuracy expected for the Lunar Orbiter missions, some calculations have been made of the sensitivities in range rate due to the influence of gravitational coefficients. These results are presented in figure 4. The plots represent the short-period differences between range rate data calculated for orbits with and without inclusion of gravitational coefficients of the magnitudes noted on the figure. The value of $C_{3,0}$ used on the plot represents a desired accuracy in this parameter in order to verify a long lifetime with the parameters of the nominal orbit, as discussed in reference 8; the values of the other coefficients represent improvements and extensions of present knowledge. An estimate of the noise level of the range rate data of 0.002 meter per second is shown on the plot as a basis for comparison.

The results shown in the figure indicate that range rate measurements within the expected accuracy of the data will allow improved determination of gravitational parameters. Cumulative effects produced in successive orbits will, of course, introduce greater perturbations than those shown, and will be utilized in the postflight analysis.

RESULTS OF SOME PRELIMINARY ANALYSES

Normal matrices for certain gravitational parameters were formed and inverted $\left(\text{i.e., } \left(A^T W A\right)^{-1}\right)$ to study the accuracy of determining the gravitational parameters and to analyze the condition of the normal matrix for inversion. In this preliminary analysis a simple model was assumed in which the moon revolves about the earth in a circular orbit and a single observation

station at the center of the earth makes uncorrelated, unbiased, range and range rate measurements of a lunar satellite. The assumed standard deviation of the tracking data was 0.002 meter per second and 10 meters for range rate and range, respectively. Both of these numbers are estimates of the DSN capability in 1966. The orbital elements of the lunar satellite considered throughout the study are typical of those for the photographic mission. Occulation of the satellite by the moon was included in order to study the aliasing effect of the lack of observations when the satellite is behind the moon. In general, occulation eliminated about one-fifth of the data points considered.

Analysis of Direct Method

For the direct method referred to earlier, the observations are related directly to the gravitational parameters through the integrals of the equations of motion of the spacecraft. Hence, in order to form the partial derivatives of the observables with respect to the gravitational parameters, which are needed to form the normal matrix, the equations of motion of the lunar satellite must be integrated by some means. For this preliminary study a first-order general perturbation method, similar to that discussed in reference 9, was utilized to obtain the desired integral of the motion. The required partial derivatives were then obtained by direct differentiation.

Figure 5 shows the standard deviations of all of the zero, first, and second degree coefficients and the third, fourth, and fifth zonal coefficients as a function of the number of consecutive orbits of tracking. Only range rate data, equally spaced in time, are considered, with a frequency of 26 observations per orbit before occulation by the moon. After just 10 orbits of tracking it is seen that a considerable improvement in the present knowledge of the

moon's mass $(C_{0,0})$, oblateness $(C_{2,0})$, and ellipticity $(C_{2,2})$ can be realized. In addition, the uncertainties in the higher degree odd zonal coefficients, which primarily determine the lifetime of the satellite, are small enough that long-period variation in pericentron altitude can be predicted to better than 10 km. Figure 6 gives the correlation matrix (i.e., the matrix of correlation coefficients) at the end of the tenth complete orbit. After this tracking period all of the very high correlations have been eliminated and even the expected correlation between the pairs $(C_{2,0},\ C_{4,0})$ and $(C_{3,0},\ C_{5,0})$ have been reduced to not unreasonably high values. Somewhat unexpected correlations appear between some of the second degree coefficients. These correlations are partly due to the particular choice of the nodal position of the lunar satellite orbit. At other nodal positions the correlations between these two pairs of coefficients are smaller, and higher correlations appear between other pairs of the second degree parameters. Even though there are no extremely high correlations, the normal matrix is not well conditioned for inversion and double precision (16 decimal digits) arithmetic should be utilized.

It should be noted that only range rate data were used to form the normal matrices discussed above. This was done because there may be some limitation on the amount of range data available, particularly during the photographic phase of the mission. Because of this possible restriction, it is of interest to compare the relative advantages of range and range rate data. The results of such a comparison are shown in figure 7. The first three columns of the table give the coefficients and the corresponding standard deviations using range rate data only and range data only. In general, the range rate data give from one to three times more accurate results than the range data. In addition, combining both types of data does not appreciably improve the condition of the

normal matrix for inversion as can be seen by comparing the correlation matrices using range rate only (fig. 6) with that shown in figure 7 where both data types are used. It is seen that those parameters which were highly correlated when only range rate data were used are still highly correlated when both types are used.

There has been some discussion, based primarily on photographic considerations, of performing the photographic mission at lower inclinations than the nominal value of 15°, and also at much higher inclinations. It is therefore of interest to study the effect of various inclinations on the accuracy of determining the parameters. Figure 8 shows the results of such a study for the direct method. The results presented are at the end of 10 consecutive orbits of tracking with Doppler data only. The standard deviations in the mass of the moon $(C_{0,0})$ and in the tesseral harmonics show no uniform variation with inclination; however, the accuracy of determining all of the zonal coefficients improves with inclination over the range of inclination considered. The condition of the matrix improves with inclination, primarily due to large reductions in correlation between the even zonal coefficients. The correlation matrices for the zonal coefficients are presented to illustrate this improvement.

Analysis of Long-Period and Secular Method

A second method which can be used to determine the gravitational coefficients employs a reduction of the observations over nonoverlapping time arcs to determine a set of "mean" elements and the covariance matrix of the mean elements. These "mean" elements become the observations in the formation of the normal equations. The observations are weighted by the inverse of the covariance matrix for each set of mean elements, while the individual sets of mean elements are assumed to be uncorrelated with any other set. The computed values of the

mean elements and the required partial derivatives come from the solution of the equations of motion retaining only the long-period and secular variations. Thus all the ingredients to form the normal equations are available.

For this preliminary analysis the covariance matrix for the "mean" elements was obtained using the simple model discussed earlier and assuming undisturbed Keplerian motion for the lunar satellite. The long-period and secular equations of motion were derived from the first-order perturbation theory used in the direct method by time-averaging the disturbing function over one orbital period. For all of the results presented here it was assumed that data were taken over two consecutive orbital periods to determine the "mean" elements.

Figure 9 shows the accuracy with which the mass of the moon, the second degree coefficients, and the third, fourth, and fifth degree zonal coefficients can be determined using range rate measurement only. The tracking accuracy and satellite orbital elements are the same as those used in the direct method. The rapid improvement in the accuracy of determining some of the parameters at certain times of the month is due to the strong dependence of the accuracy of determining the state variables of the satellite on the nodal position of the satellite orbit relative to the earth-moon line.

Figure 10 gives the corresponding correlation matrix at the end of 30 days. The only remaining high correlation is between the two higher degree odd zonal coefficients $C_{3,0}$ and $C_{5,0}$. This correlation appears because these two harmonics cause long-period variation in all the elements except the semimajor axis. For a lunar satellite the eccentricity can be determined with considerably better accuracy than the angular elements and hence it is only the relatively inaccurate angular data which allow any separation at all between these two zonal coefficients. This correlation matrix after 30 days is well conditioned for

inversion with single precision arithmetic (8 decimal digits); however, during the first few days of the reduction the adequacy of single precision is questionable.

As in the direct method, range and range rate data were compared and figure 11 shows the results of this comparison. Utilizing range rate data only results in an improvement of a factor of two over using range data only. As in the direct method there are no important reductions in the correlations between coefficients or improvement in the condition of the covariance matrix by using both types of data.

CONCLUDING REMARKS

The analyses described above will be extended in the next few months to include consideration of higher degree gravitational coefficients and instrument and measurement biases. These present and future studies should provide a good assessment of gravitational parameter accuracies which will be obtained from the actual tracking data from the Lunar Orbiter.

ACKNOWLEDGMENT

The authors wish to express their appreciation for contributions to this paper by members of the Langley Research Center, particularly Messrs. H. C. Compton and W. R. Wells of the Space Mechanics Division.

REFERENCES

1. Taback, I.; and Brummer, E. A.: The Lunar Orbiter. Presented at the AIAA Unmanned Spacecraft Meeting, Los Angeles, California, Mar. 1965. (Also published as NASA TM X-56116.)

2. Sjogren, W. L.; et al.: The Ranger VI Flight Path and Its Determination From Tracking Data. Tech. Rept. No. 32-605, Jet Prop. Lab., C.I.T., Dec. 15, 1964.

3. Wollenhaupt, W. R.; et al.: Ranger VII Flight Path and Its Determination From Tracking Data. Tech. Rept. No. 32-694, Jet Prop. Lab., C.I.T., Dec. 15, 1964.

4. Kaula, W. M.: The Investigation of the Gravitational Fields of the Moon and Planets With Artificial Satellites. Advances in Space Science and Technology, Vol. 5, Academic Press, Inc., New York, 1963.

5. Kaula, W. M.: Determination of the Earth's Gravitational Field. Review of Geophysics, vol. 1, no. 4, Nov. 1963.

6. Anderson, J. D.; Null, G. W.; and Thornton, C. T.: The Evaluation of Certain Astronomical Constants From the Radio Tracking of Mariner II. Progress in Astronautics and Aeronautics, Vol. 14, Academic Press, Inc., New York, 1964.

7. Clarke, V. C., Jr.: Constants and Related Data for Use in Trajectory Calculations. Tech. Rept. No. 32-604, Jet Prop. Lab., C.I.T., Mar. 6, 1964.

8. Wells, W. R.: Analytical Lifetime Studies of a Near-Lunar Satellite. NASA TN D-2805, 1965.

9. Kaula, W. M.: Analysis of Gravitational and Geometric Aspects of Geodetic Utilization of Satellites. Geophysical Jour. of the Astronomical Soc., May 1961.

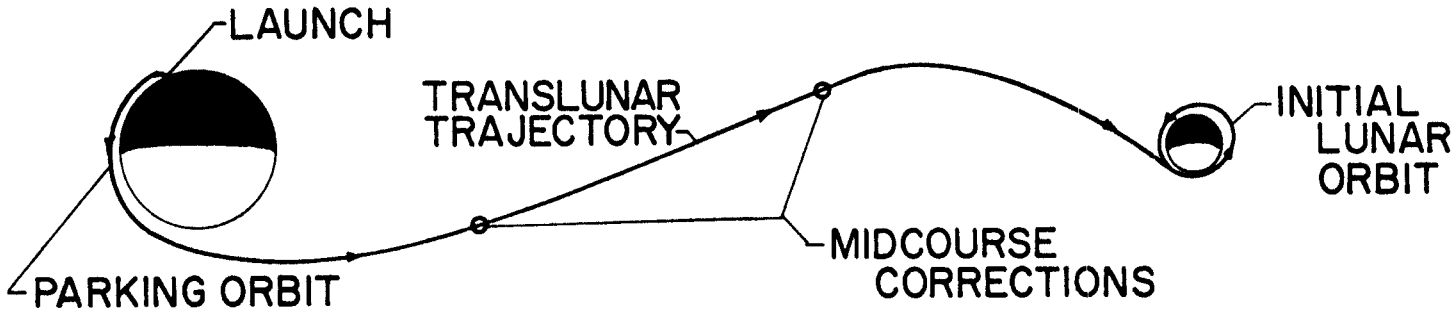

a=2686KM
e=0.336
i=15°
p=3.5HR

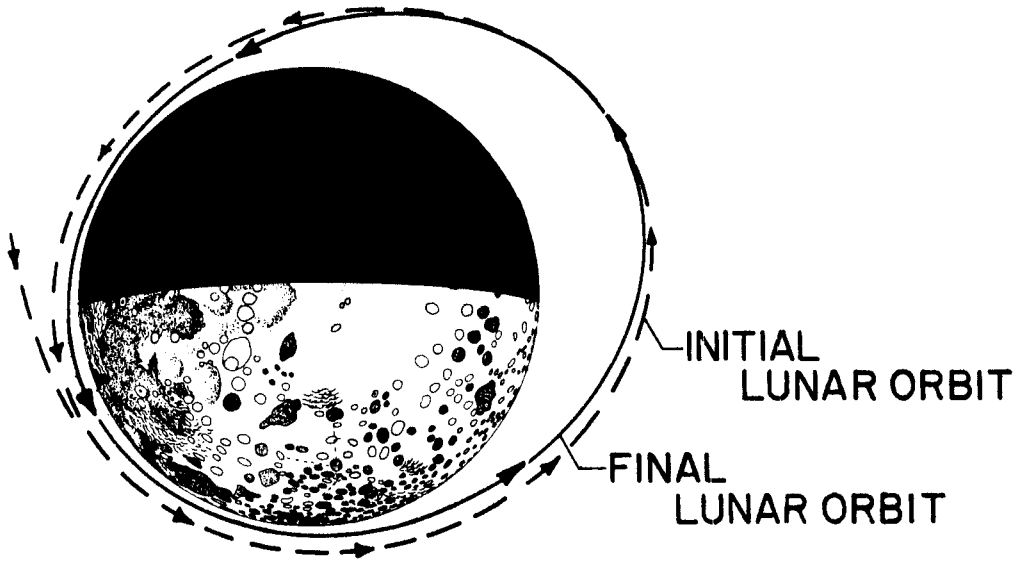

NASA

Figure 1.- Mission profile.

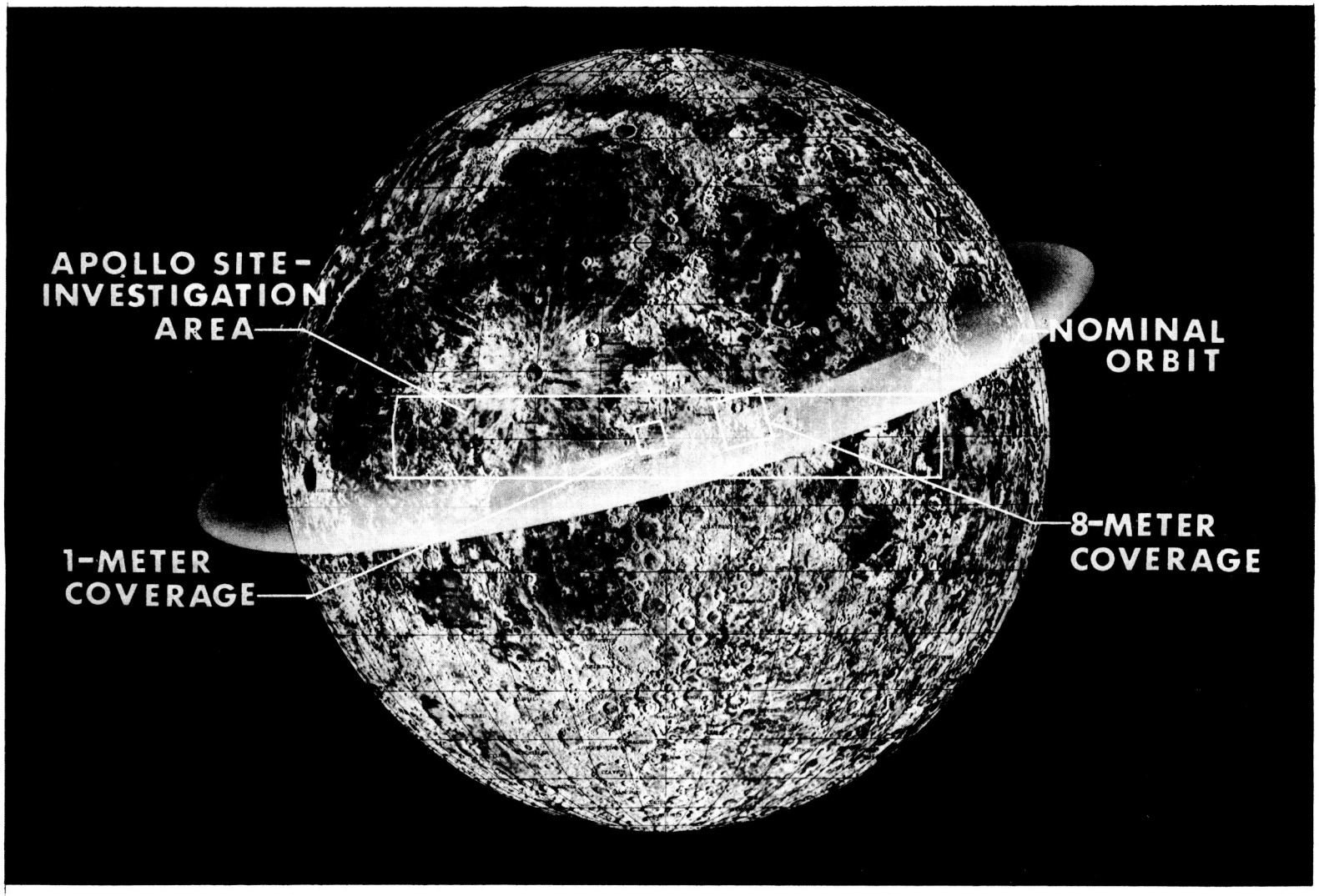

NASA

Figure 2.- Photographic coverage.

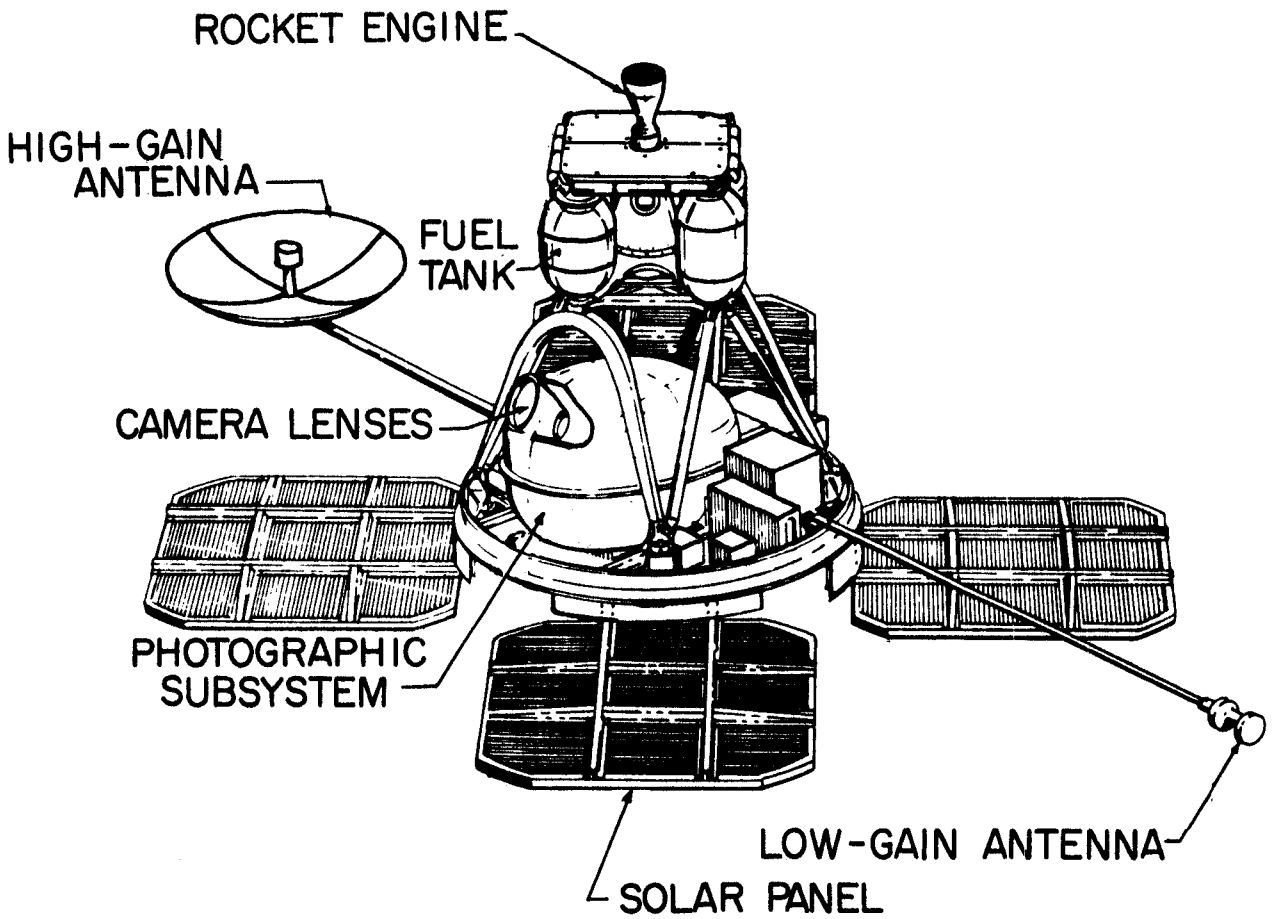

Figure 3.- Spacecraft configuration.

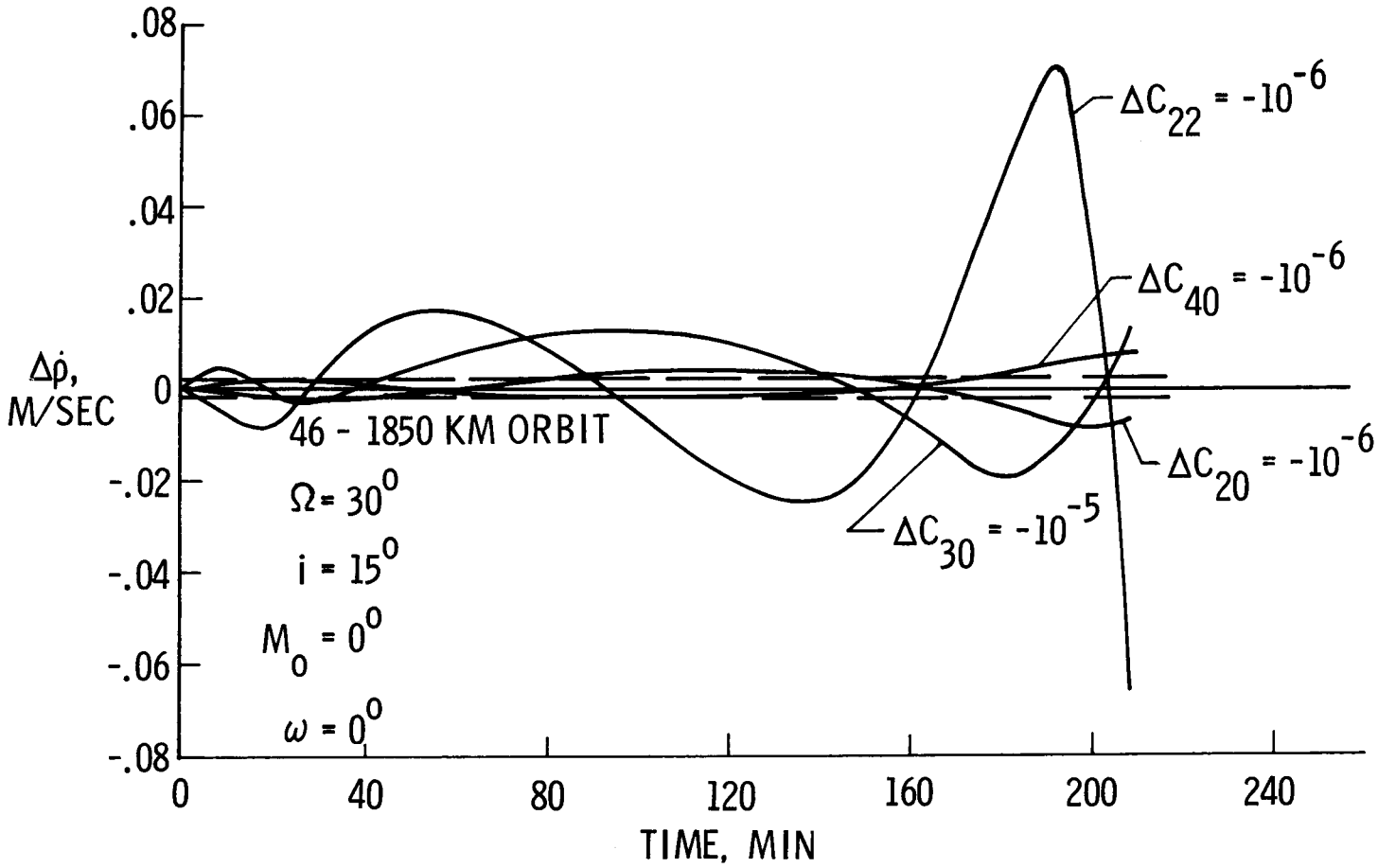

Figure 4.- Short-period sensitivities in range rate data.

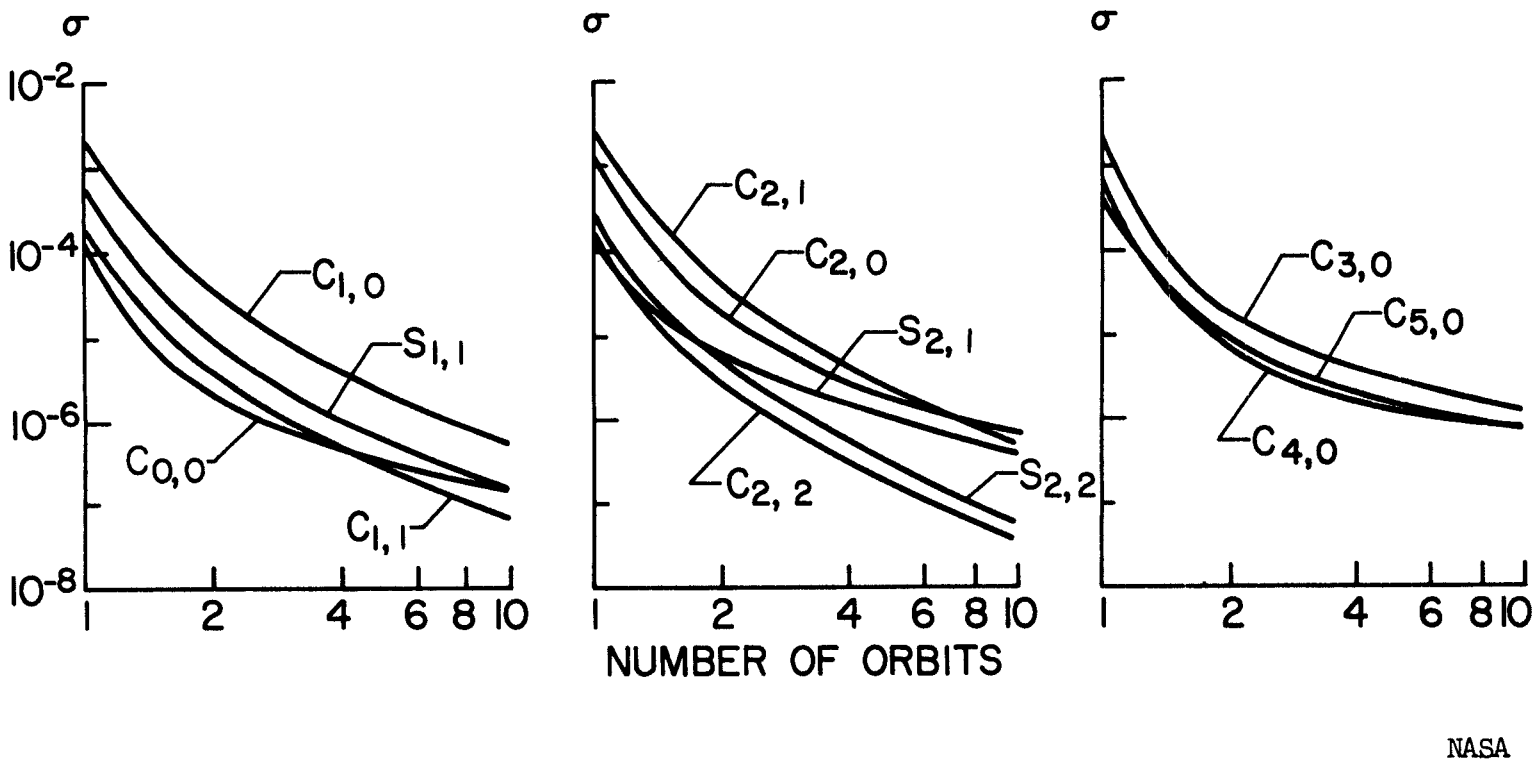

Figure 5.- Accuracy of the determination of gravitational parameters for 10 consecutive orbits using the direct method.

$a = 2686$ KM; $e = 0.336$; $i = 15^0$; $\Omega = 30^0$; $\omega^0 = 0^0$; $\sigma_\rho = 0.002$ m/s;

26 RANGE-RATE MEASUREMENTS PER ORBIT EQUALLY SPACED IN TIME

	$C_{0,0}$	$C_{1,0}$	$C_{1,1}$	$C_{2,0}$	$C_{2,1}$	$C_{2,2}$	$C_{3,0}$	$C_{4,0}$	$C_{5,0}$	$S_{1,1}$	$S_{2,1}$	$S_{2,2}$
$C_{0,0}$	1.00	-.14	.35	.21	.11	-.11	-.10	-.03	.01	-.03	-.30	-.18
$C_{1,0}$		1.00	-.01	.44	-.03	.17	.55	.55	.61	-.27	.39	.13
$C_{1,1}$			1.00	.07	-.60	-.50	-.62	-.20	-.48	-.66	-.41	.39
$C_{2,0}$				1.00	-.07	.64	.49	.87*	.55	.18	.78	.07
$C_{2,1}$					1.00	.39	.51	.38	.40	.60	.15	-.94*
$C_{2,2}$						1.00	.53	.68	.52	.42	.88*	-.18
$C_{3,0}$							1.00	.59	.93*	.63	.63	-.25
$C_{4,0}$								1.00	.63	.17	.77	-.26
$C_{5,0}$									1.00	.44	.60	-.20
$S_{1,1}$										1.00	.38	-.37
$S_{2,1}$											1.00	.11
$S_{2,2}$												1.00

*ABSOLUTE VALUE GREATER THAN 0.85

NASA

Figure 6.- Correlation matrix after 10 consecutive orbits.

26 MEASUREMENTS PER ORBIT; σ_ρ = 10 m; $\sigma_{\dot\rho}$ = 0.002 m/sec

	$\sigma \times 10^7$		CORRELATION MATRIX AFTER TEN ORBITS USING BOTH RANGE AND RANGE-RATE MEASUREMENTS										
	RANGE RATE	RANGE	$C_{0,0}$	$C_{1,0}$	$C_{1,1}$	$C_{2,0}$	$C_{2,1}$	$C_{2,2}$	$C_{3,0}$	$C_{4,0}$	$C_{5,0}$	$S_{1,1}$	$S_{2,1}$	$S_{2,2}$
$C_{0,0}$	1.506	4.749	1.00	-.24	.52	-.02	.02	-.32	-.36	-.29	-.25	-.16	-.53	-.19
$C_{1,0}$	4.952	8.540		1.00	.07	.42	-.07	.08	.53	.54	.58	-.39	.33	.17
$C_{1,1}$	0.779	1.198			1.00	.09	-.53	-.49	-.57	-.12	-.35	-.66	-.46	.24
$C_{2,0}$	7.510	11.539				1.00	.03	.64	.42	.88*	.54	.03	.75	.09
$C_{2,1}$	4.754	6.063					1.00	.32	.43	.24	.20	.57	.15	-.90*
$C_{2,2}$	0.379	0.786						1.00	.47	.63	.43	.40	.91*	-.04
$C_{3,0}$	13.839	19.360							1.00	.50	.88*	.55	.62	-.10
$C_{4,0}$	8.267	17.431								1.00	.58	-.01	.77	-.15
$C_{5,0}$	8.122	8.897									1.00	.30	.58	.01
$S_{1,1}$	1.554	2.539										1.00	.34	-.28
$S_{2,1}$	4.003	9.536											1.00	.15
$S_{2,2}$	0.556	0.538												1.00

*ABSOLUTE VALUE GREATER THAN 0.85

NASA

Figure 7.- Comparison of accuracy of determining the gravitational parameters from range and range rate measurements.

a = 2686 KM; e = 0.336; $\Omega = 30^0$; $\omega = 0^0$; $\sigma_{\dot{\rho}} = 0.002$ m/s;

26 RANGE-RATE MEASUREMENTS PER ORBIT EQUALLY SPACED IN TIME

INCLINATION, DEG	$\sigma \times 10^7$											
	$C_{0,0}$	$C_{1,0}$	$C_{1,1}$	$C_{2,0}$	$C_{2,1}$	$C_{2,2}$	$C_{3,0}$	$C_{4,0}$	$C_{5,0}$	$S_{1,1}$	$S_{2,1}$	$S_{2,2}$
5	3.63	13.46	0.72	15.13	13.68	0.30	25.57	13.92	14.50	1.47	9.21	0.56
15	1.51	4.95	0.78	7.51	4.75	0.38	13.84	8.27	8.12	1.55	4.00	0.56
50	1.71	1.02	0.70	1.87	0.97	0.61	2.08	1.99	3.18	1.13	1.86	0.54

	$i = 5^0$						$i = 15^0$						$i = 50^0$					
	$C_{0,0}$	$C_{1,0}$	$C_{2,0}$	$C_{3,0}$	$C_{4,0}$	$C_{5,0}$	$C_{0,0}$	$C_{1,0}$	$C_{2,0}$	$C_{3,0}$	$C_{4,0}$	$C_{5,0}$	$C_{0,0}$	$C_{1,0}$	$C_{2,0}$	$C_{3,0}$	$C_{4,0}$	$C_{5,0}$
$C_{0,0}$	1.00	.19	.93*	.09	.91*	.05	1.00	-.14	.21	-.10	-.03	.01	1.00	-.22	-.03	.02	-.24	-.22
$C_{1,0}$		1.00	.22	.26	.25	.36		1.00	.44	.55	.55	.61		1.00	-.33	.43	-.40	.39
$C_{2,0}$			1.00	.10	.96*	-.01			1.00	.49	.87*	.55			1.00	-.44	.47	-.25
$C_{3,0}$				1.00	.11	.83				1.00	.59	.93*				1.00	-.86*	.81
$C_{4,0}$					1.00	-.02					1.00	.63					1.00	-.60
$C_{5,0}$						1.00						1.00						1.00

*ABSOLUTE VALUE GREATER THAN 0.85

NASA

Figure 8.- Accuracy of determining the gravitational parameters at different inclinations.

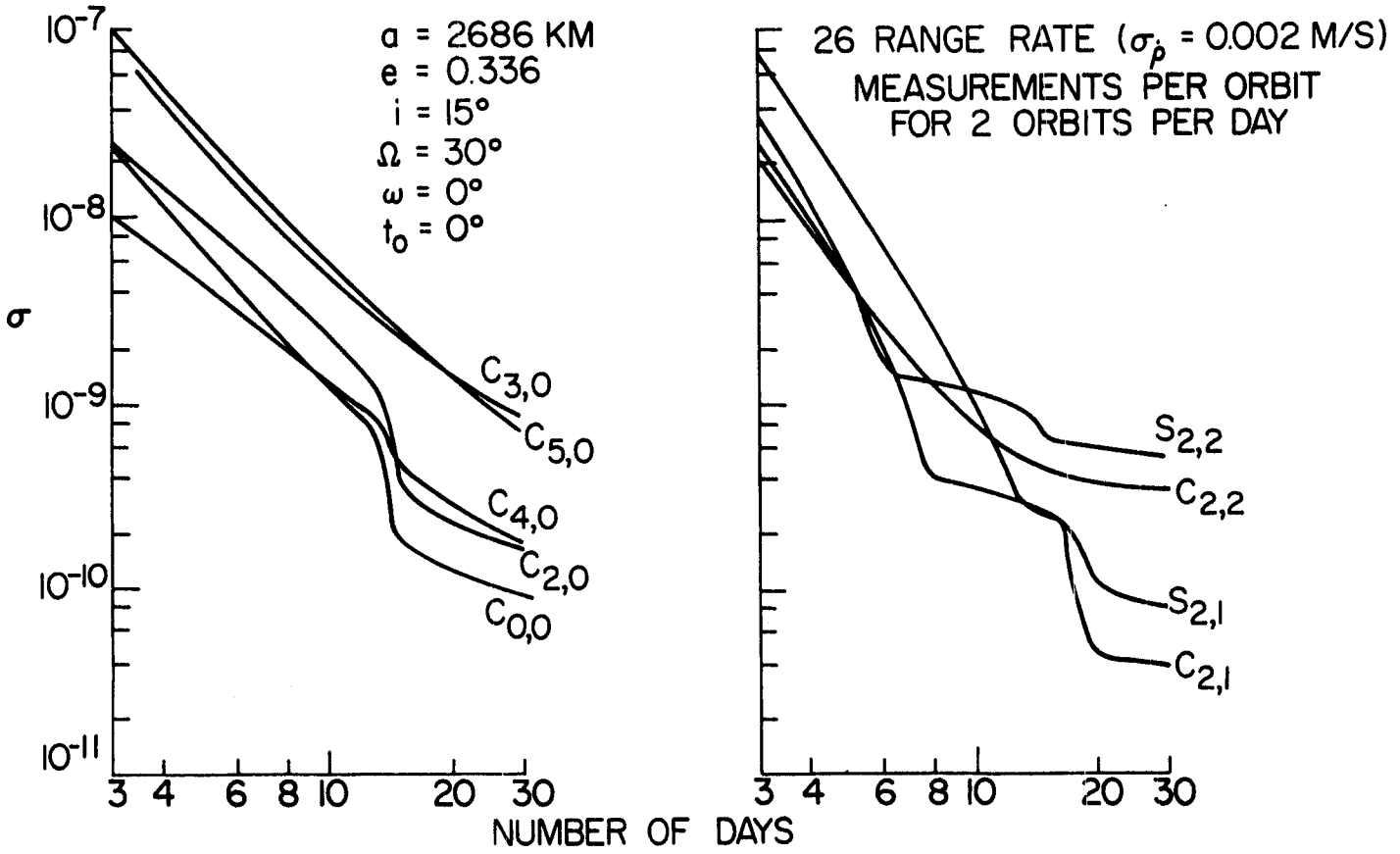

NASA

Figure 9.- Accuracy of determination of gravitational parameters by secular and long-period variations in orbital elements.

$a = 2686$ KM; $i = 15^0$; $\Omega = 30^0$; $\omega = 0^0$; $e = 0.336$; $t_0 = 0$; $\sigma_{\dot{\rho}} = 0.002$ m/s

	$C_{0,0}$	$C_{2,0}$	$C_{2,1}$	$C_{2,2}$	$C_{3,0}$	$C_{4,0}$	$C_{5,0}$	$S_{2,1}$	$S_{2,2}$
$C_{0,0}$	1.00	.62	-.06	-.46	.11	.08	.13	-.01	.10
$C_{2,0}$		1.00	-.15	-.30	.02	.72	.12	.11	-.12
$C_{2,1}$			1.00	.07	-.13	-.19	-.51	-.63	.14
$C_{2,2}$				1.00	-.03	.18	-.08	.10	-.18
$C_{3,0}$					1.00	.00	.88*	.09	.04
$C_{4,0}$						1.00	.15	.29	-.43
$C_{5,0}$							1.00	.33	-.09
$S_{2,1}$								1.00	-.14
$S_{2,2}$									1.00

*ABSOLUTE VALUE GREATER THAN 0.85

NASA

Figure 10.- Correlation matrix after 30 days - two orbits per day.

2 ORBITS PER DAY AT 26 MEASUREMENTS PER ORBIT
σ_ρ = 10 m, $\sigma_{\dot\rho}$ = 0.002 m/s

	$\sigma \times 10^{10}$		CORRELATION MATRIX USING BOTH RANGE AND RANGE-RATE MEASUREMENTS								
	RANGE RATE	RANGE	$C_{0,0}$	$C_{2,0}$	$C_{2,1}$	$C_{2,2}$	$C_{3,0}$	$C_{4,0}$	$C_{5,0}$	$S_{2,1}$	$S_{2,2}$
$C_{0,0}$	0.890	2.167	1.00	.64	-.05	-.45	.09	.12	.12	-.01	.11
$C_{2,0}$	1.712	3.887		1.00	-.13	-.29	.02	.72	.12	.11	-.11
$C_{2,1}$	0.348	0.771			1.00	-.06	-.13	-.18	-.54	-.62	.14
$C_{2,2}$	3.801	6.905				1.00	-.03	.17	-.07	.10	-.18
$C_{3,0}$	8.136	10.856					1.00	.00	.85*	.09	.04
$C_{4,0}$	1.818	3.668						1.00	.16	.27	-.43
$C_{5,0}$	6.989	11.167							1.00	.35	-.09
$S_{2,1}$	0.856	1.754								1.00	-.14
$S_{2,2}$	5.426	10.538									1.00

*ABSOLUTE VALUE GREATER THAN 0.85

NASA

Figure 11.- Comparison of accuracy of determining the gravitational parameters from range and range rate measurements after 30 days.